

RESEARCH PAPER



The PRC2 complex directly regulates the cell cycle and controls proliferation in skeletal muscle

Abhinav Adhikari  and Judith K. Davie 

Department of Biochemistry and Molecular Biology and Simmons Cancer Institute, Southern Illinois University School of Medicine, Carbondale, IL, USA

ABSTRACT

The polycomb repressive complex 2 (PRC2) is an important developmental regulator responsible for the methylation of histone 3 lysine 27 (H3K27). Here, we show that the PRC2 complex regulates the cell cycle in skeletal muscle cells to control proliferation and mitotic exit. Depletions of the catalytic subunit of the PRC2 complex, EZH2, have shown that EZH2 is required for cell viability, suggesting that EZH2 promotes proliferation. We found that EZH2 directly represses both positive and negative cell cycle genes, thus enabling the PRC2 complex to tightly control the cell cycle. We show that modest inhibition or depletion of EZH2 leads to enhanced proliferation and an accumulation of cells in S phase. This effect is mediated by direct repression of cyclin D1 (*Ccnd1*) and cyclin E1 (*Ccne1*) by the PRC2 complex. Our results show that PRC2 has pleiotropic effects on proliferation as it serves to restrain cell growth, yet clearly has a function required for cell viability as well. Intriguingly, we also find that the retinoblastoma protein gene (*Rb1*) is a direct target of the PRC2 complex. However, modest depletion of EZH2 is not sufficient to maintain *Rb1* expression, indicating that the PRC2 dependent upregulation of cyclin D1 is sufficient to inhibit *Rb1* expression. Taken together, our results show that the PRC2 complex regulates skeletal muscle proliferation in a complex manner that involves the repression of *Ccnd1* and *Ccne1*, thus restraining proliferation, and the repression of *Rb1*, which is required for mitotic exit and terminal differentiation.

ARTICLE HISTORY

Received 31 October 2019
Revised 1 July 2020
Accepted 28 July 2020

KEYWORDS

EZH2; PRC2; cyclin D1; cyclin E1; retinoblastoma protein (pRB, RB1); skeletal muscle; cell cycle

Introduction

Skeletal muscle proliferation and differentiation are closely coordinated and highly regulated processes. Myogenesis is a multistep process which involves the determination of multi-potential mesodermal cells that give rise to myoblasts; withdrawal of the myoblasts from the cell cycle and finally, the differentiation of myoblasts into muscle fibers [1,2]. A complex network of cell cycle effector genes goes from highly expressed to permanently silenced as myoblasts differentiate into myotubes, while another set of genes which are normally repressed in myoblasts become activated in myotubes [3]. Skeletal muscle determination and differentiation are controlled by four highly related basic-helix-loop-helix (bHLH) transcription factors known as the myogenic regulatory factors (MRFs) which include Myf5 (*Myf5*), MyoD (*Myod1*), myogenin (*Myog*) and Mrf4 (*Myf6*) [4–6].

Two important protein families involved in the cell cycle machinery are cyclins and cyclin-dependent kinases (CDKs). These complexes orchestrate the advance of the cell cycle through different phases. In mammals, cyclin D and E mediate the progression through G1/S phases [7]. The mitotic cyclins A and B mediate progression through the S/G2/M phases. D-type cyclins are short-lived proteins whose synthesis and assembly with CDK4 or CDK6 are dependent on mitogenic signaling [8]. Cyclin D drives cell cycle progression through the phosphorylation of critical cellular substrates. In addition, D type cyclins play a kinase-independent role by sequestering the CDK inhibitors p27^{kip1} and p21^{cip1} [7]. The cyclin E protein level peaks at the G1/S progression, followed by an increase in cyclin A levels in S-phase. CDK2 can form complexes with both cyclin A and E, whereas CDK1 can only form a complex with cyclin A. An increase in cyclin

CONTACT Judith K. Davie  jdavie@siumed.edu

 Supplemental data of this article can be accessed [here](#).

B levels results in the induction of CDK1 levels at the G2/M phase. The resultant fluctuation in expression of cyclins and oscillation of CDKs activities forms the basis of coordinated cell cycle progression (reviewed in [3]).

The retinoblastoma protein (pRB) plays a central role in negatively regulating cell cycle progression by promoting cell cycle exit and maintenance of the differentiated state [9,10]. Cell cycle arrest is a critical step for muscle differentiation. pRB maintains cell cycle arrest in part by regulating the activity of the E2F family of transcription factors. Activator E2F is repressed through binding to pocket proteins, a family that includes pRB as well as related p107 and p130 proteins [11]. Under mitogen rich conditions, growth factors override the repressive action of pocket proteins through activation of cyclin D1 and CDK4/6 proteins, which phosphorylate the pocket proteins, leading to the release of bound activator E2F transcription factors [12]. This results in the activation of E2F target cell cycle genes, including cyclin E, which in complex with CDK2 further hyper-phosphorylates pRB proteins, leading to progression of cells through the G1/S restriction point [13]. Modification of the chromatin environment through the recruitment of repressor proteins, such as histone deacetylases (HDAC) and the PRC2 complex, by the pRB family of pocket proteins is an important mechanism by which the pRB family of proteins repress transcription [10].

Polycomb repressor proteins have important developmental roles and play essential roles in skeletal muscle specification. The two major polycomb complexes, Polycomb Repressive Complex 1 (PRC1) and Polycomb Repressive Complex 2 (PRC2), are responsible for the ubiquitination of lysine 119 of histone H2A (H2AK119) [14] and the methylation of lysine 27 on histone H3 tail (H3K27), respectively [15–17]. Methylation of H3K27 recruits PRC1, which then catalyzes the ubiquitinylation of H2AK119. The methylation of H3K27 by PRC2 requires one of the enhancer of zeste proteins, EZH1 or EZH2. Promoters and enhancers of many lineage-specific genes contain di- and tri-methylated H3K27, and many of these

genes lose the methylation profile upon differentiation (reviewed in [18]).

The PRC2 complex has been shown to be required for proliferation in several cell types [10] and has been implicated in muscle stem cell (MSC) viability as well [19,20]. In MSCs, the PRC2 complex represses the expression of PAX7, a transcription factor implicated in control of the specification [21], renewal [22] and cell cycle exit of MSCs [23]. In MSCs, PAX7 is repressed by inflammatory signaling by TNF- α , which activates p38 and leads to p38 mediated PRC2 repression [24,25]. Intriguingly, this mechanism only occurs in MSCs as PAX7 is unresponsive to p38 signaling but constitutively repressed by PRC2 in myotubes [24]. TNF- α has also been shown to repress Notch-1 through the recruitment of PRC2 and DNA methyltransferases [26].

The PRC2 complex has also been implicated in the repression of cyclin D1 (*Ccnd1*). *Ccnd1* has been shown to be H3K27 methylated by PRC2 in neural cells [27] and in leukemia [28]. *Ccnd1* has also been found to be H3K27 methylated in skeletal muscle myotubes when *Ccnd1* is not normally expressed [10]. PRC2 has also been shown to repress *Ccne1* in oocytes [29].

We have recently shown that loss of the PRC2 complex blocks differentiation in C2C12 cells through modulation of the canonical Wnt signaling pathway [30]. Differentiation and proliferation are mutually exclusive processes, thus, here we examined the effect of the PRC2 complex on the proliferation of skeletal muscle cells. Unexpectedly, we found that a modest depletion or inhibition of EZH2 increased the proliferation rate and caused the derepression of the positive cell cycle regulators cyclin D1 and cyclin E1, while the negative cell cycle regulator pRB was inactivated by phosphorylation and downregulated. Transient depletion of EZH2 led to cells which either actively proliferated or induced apoptosis, suggesting a dual effect for EZH2. Chemical inhibition of EZH2 confirmed that modest inhibition of EZH2 relieves repression of cyclin D1 and cyclin E1 and promotes proliferation, while severe inhibition leads to a reduction in cell viability. EZH2's ability to repress

proliferation is dependent on JARID2, which recruits EZH2 to the promoters of *Ccnd1* and *Ccne1* [31]. Thus, PRC2 has a dual role in controlling proliferation in skeletal muscle, and the overall level of EZH2 in cells is a profound determinant of cell fate.

Materials and methods

Cell culture

C2C12 cells (ATCC) were grown in Dulbecco's modified Eagle medium (DMEM) supplemented with 10% fetal bovine serum (Hyclone) according to standard protocols. Proliferating C2C12 myoblasts were grown in DMEM supplemented with 10% fetal bovine serum (FBS, Hyclone). Primary myoblasts were isolated according to standard protocols [32]. Briefly, hindlimb muscle of the neonate mice were isolated, digested with Collagenase Type II (Worthington). The cells were filtered through sterile 70-micron filter, plated on gelatin-coated plates in 20% FBS in F-10 basal media with 1X Penicillin-Streptomycin (Corning) and 2.5 ng/ml bFGF (gift of D. Cornelison, University of Missouri). Primary myoblasts were enriched on every passage afterward by pre-plating cells on to uncoated plates for 30 min before transferring the myoblast suspensions onto collagen-coated plates. It was repeated until the majority of the cells were primary myoblasts. Myoblast identity was confirmed by expression analysis of MRFs, differentiation assay, and staining. All mouse procedures were approved by the SIU Institutional Animal Care and Use Committee.

shRNA knock down

EZH2 was depleted with shRNA constructs designed by the RNAi Consortium in the pLOK.1 plasmid (Open Biosystems) as described [30]. Three constructs targeting murine *Ezh2* and one scrambled control were linearized using the *ScaI* restriction enzyme (New England Biolabs), transfected into C2C12 cells, and selected with puromycin (2 μ g/ml). Individual clones were selected, propagated, and confirmed by mRNA

and protein analysis. For the transient depletions, the shRNA plasmids were transfected using Turbofect as described earlier without linearization. The mRNA and protein were extracted and assayed at the indicated time points. No drug selection was used in transient depletion experiments.

Western blot analysis

Cell extracts were made by lysing PBS washed cell pellets in radio-immunoprecipitation assay buffer (RIPA) supplemented with protease inhibitors (Complete protease inhibitor, Roche Diagnostics). Following incubation on ice, clear lysates were obtained by centrifugation. Protein concentrations were determined by Bradford's assay (Bio-Rad). For each sample, 30 μ g of protein was loaded on each gel unless otherwise specified. Proteins were transferred onto a PVDF membrane using a tank blotter (Bio-Rad). The membranes were then blocked with 5% milk in 1X Tris-buffered saline plus tween 20 (TBST) and incubated with primary antibody overnight at 4°C. Membranes were then washed with 1X TBST and incubated with the corresponding secondary antibody. Membranes were again washed with 1X TBST, incubated with chemiluminescent substrate according to manufacturer's protocol (SuperSignal, Pierce) and visualized by autoradiography or an iBright Imaging System. The antibodies used include anti-EZH2 (Cell Signaling), anti-cyclinD1 (DCS-6, Biolegend), anti-cyclin E1 (SCBT), anti-CDK2 (ABclonal), anti-CDK4 (ABclonal), anti-pRB1 (LabVision), anti-p21 (ABclonal), anti-phospho RB1(T821) (ab4787, Abcam), anti-Tubulin (E7, DSHB) and anti-GAPDH (Millipore). Protein expression levels were quantified using ImageJ (NIH) or iBright analysis software on at least three independent experiments. Representative images are shown.

Quantitative real-time PCR

RNA was isolated from cells by Trizol extractions (Invitrogen). Following treatment with DNase

(Promega), two micrograms of total RNA was reversed transcribed with MultiScribe™ MuLV reverse transcriptase (Applied Biosystems). cDNA equivalent to 40 ng was used for quantitative polymerase chain reaction (qPCR) amplification (Applied Biosystems) with SYBR green PCR master mix (Applied Biosystems). Samples in which no reverse transcriptase was added (no RT) were included for each RNA sample. qPCR data were calculated using the comparative Ct method (Applied Biosystems). Standard deviations from the mean of the [Δ] Ct values were calculated from three independent RNA samples. Primers are described in Supplemental Table 1. Where possible, intron spanning primers were used. All quantitative PCR was performed in triplicate, and three independent RNA samples were assayed for each time point. For measurements of relative gene expression, a fold change was calculated for each sample pair and then normalized to the fold change observed at HPRT and/or 18S rRNA.

Chromatin immunoprecipitation assays

ChIP assays were performed as described previously [33]. The following antibodies were used: anti-Jarid2 (Cell Signaling), anti-Ezh2 (Cell Signaling), anti-H3K27me3 (Cell Signaling) and anti-H3K9me (pan)(Cell Signaling). Rabbit IgG (SCBT) was used as a nonspecific control. Primers are described in Supplemental Table 1. Primers to detect H3K27 methylation were designed based on the H3K37 methylation peaks detected in C2C12 cells using the WashU epigenome browser (<https://epigenomegateway.wustl.edu/>). The real-time PCR was performed in triplicate. The results were represented as the percentage of IP over input signal (% Input) with background signal subtracted. The sample variation was corrected by normalized values obtained from 2% input (1/50th) of the input chromatin (Relative Enrichment (% Input)). All ChIP assays shown are representative of at least three individual experiments. Standard error from the mean was calculated and plotted as the error bar.

EdU incorporation assay

Cells were assayed using a Click-iT EdU Alexa Flour 488 Imaging Kit according to the manufacture's protocol (Life Technologies). C2C12 and primary myoblast cells were grown in the presence of 10 μ M EdU for two and three hours, respectively, except for Figure 1(d) where C2C12 cells were grown in presence of EdU for 12 hours. Primary antibodies for EZH2 (Cell Signaling) and cleaved caspase-3 (Cell Signaling) were used to perform the immunofluorescence. Alexa Fluor 594 was used to detect the immunostained proteins. EdU and immunostained protein positive nuclei were counted in at least five random fields on microscopic images taken at 200X and 400X magnification using a Leica microscope. The signal intensity of EdU positive nuclei were measured using ImageJ software (NIH) in at least six random fields.

Proliferation assay

An equal number of cells were seeded, and on the indicated days, cells were harvested using trypsin, resuspended and counted under a light microscope using a hemocytometer. Cell viability was determined by trypan blue staining. Cell counting was performed in duplicate for at least three blinded biological replicates.

Cell cycle analysis by flow cytometry

Cells were split in 100 mm diameter plate at 1:5 dilution, grown for 48 hours in duplicates in 10% FBS in 5% CO₂ incubator. The cell plates were washed twice with sterile 1x PBS pH 7.4, harvested using trypsin, and resuspended in 1x PBS pH 7.4. Cells were pelleted down at 600x g for 5 min at room temperature (RT), washed twice with 1X PBS and were fixed in chilled 70% ethanol overnight at -20°C. Cells were washed with 1X PBS pH 7.4, treated with RNase (10 μ g/ml) and stained with propidium iodide (50 μ g/ml) for 2 hours at RT before running through a BD Accuri C6 flow cytometer (BD Biosciences, San Jose, CA). Data were analyzed using FlowJo (FlowJo LLC) software.

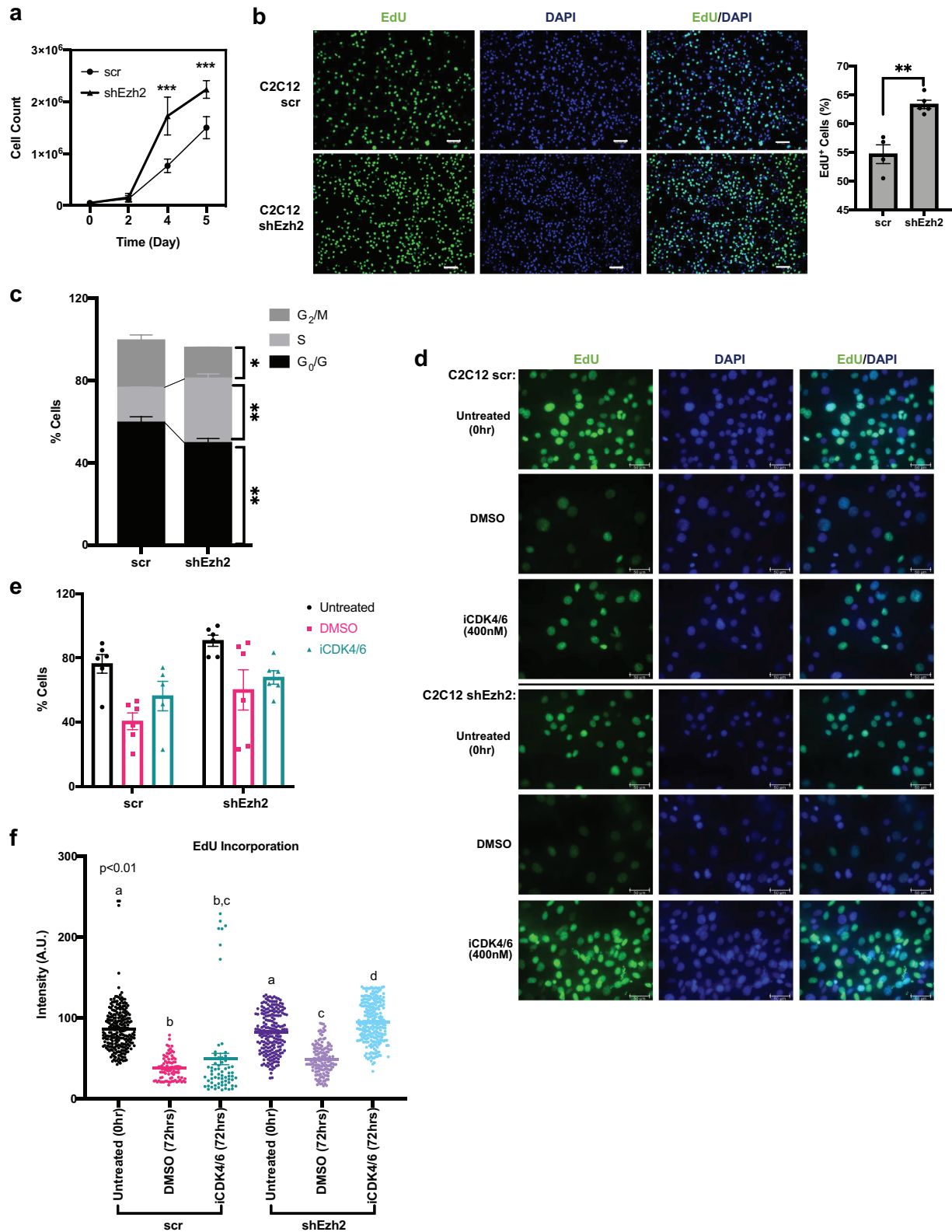


Figure 1. Stable EZH2 depletion results in increased proliferation and DNA synthesis in C2C12 cells.

a. Depletion of EZH2 increases cell proliferation. Proliferation curve for C2C12 cells stably expressing control scrambled shRNA (scr) or shRNA targeted against EZH2 mRNA (shEzh2). Data plotted are mean (\pm SEM) (Student t.test, *** $p < 0.001$, $n = 3$ biological replicates). b. Increased DNA synthesis upon depletion of EZH2 in C2C12 cells. Cells as in a. were subjected to EdU (Green) incorporation assay (left panel). DAPI (Blue) was used to stain nuclei. Scale bars, 100 μ m. Percent of EdU⁺ nuclei were counted in at least five random fields of one representative experiment of two and plotted (right panel). Data plotted are mean (\pm SEM) (Student

MTT assay

C2C12 and primary myoblast cells were harvested using trypsin and counted using a hemocytometer after trypan blue staining. 1,000 cells/well (C2C12) and 2,000 cells/well (primary myoblasts) were seeded in triplicate in 96-well plates for each concentration and time point. Wells were coated with collagen (0.01% Collagen Type I, Corning) for primary myoblasts. DMSO and GSK126 were serially diluted to the desired concentration in DMEM with 10% FBS for C2C12 and F-10 media with 20% FBS for primary myoblasts for the indicated time points. On the final day, 68 hours from the first treatment, MTT reagent was added to each well (5 mg/ml) concentration, and cells were incubated for 3 hours at 37°C in 5% CO₂ incubator. Cells were lysed with DMSO and absorbance was read at 560 nm in a multi-well plate reader (GLOMAX Multi-Detection System, Promega). GSK126 treated samples were normalized with the DMSO control samples of the same time point, and the graph was generated using GraphPad Prism 8.0. The experiment was repeated three times (n = 3).

Statistics

Data are presented as means ± standard errors (S.E.). Each dot in the bar graph represents an individual data point. Statistical comparisons were performed using the unpaired two-tailed Student's *t*-test or the ANOVA test followed by Tukey's multiple comparisons test (Figure 1(f)). Samples not sharing an alphabet are statistically significant. A probability value of <0.05 was taken to indicate significance.

Results

Modest depletion of EZH2 enhances proliferation

In a previous study, we established stable cell lines depleted for EZH2 with three independent shRNA constructs in C2C12 cells, a well established *in vitro* differentiation model [30]. In that work, we found that the loss of PRC2 dependent repression of a Wnt antagonist, *SFRP1*, resulted in impaired differentiation [30]. Here, we sought to understand the function of EZH2 in skeletal muscle proliferation. EZH2 has been shown to be required for the viability of several cell types [34] and ablation of *Ezh2* in skeletal muscle precursors led to reductions in the MSC pool [19]. Thus, we sought to determine how EZH2 controls cell proliferation in myoblasts. All described experiments were performed in cell lines depleted with two independent shRNA constructs (shEZH2-1 and shEZH2-3), and the results were consistent. Confirmation of the depletions at the RNA and protein levels are shown in Supplemental Figure 1. For clarity, only the results for one shRNA construct (shEZH2-1) are shown. We assayed for the proliferation rate of these cells, and we found that C2C12 cells depleted for EZH2 proliferated significantly faster than cells with the scrambled control (Figure 1(a)). To determine if the enhanced proliferation was correlated with increased DNA synthesis, we utilized an EdU incorporation assay and found that the number of cells with active DNA synthesis marked by EdU incorporation was significantly higher in EZH2 depleted cells (Figure 1(b)). To understand how enhanced proliferation and DNA synthesis correlated with changes in the cell cycle, we assessed the cell cycle state. We found that EZH2 depleted cells were highly enriched in S phase with

t.test, **p < 0.01, n = 2 biological replicates).c. Asynchronously growing C2C12 cells as in a. were sorted using flow cytometer after propidium iodide staining and were analyzed for cell cycle phase distribution using FlowJo software (Fig S2). Data shown are mean (±SEM) (Student t.test, *p < 0.05, **p < 0.01, n = 3 biological replicates).d-e. Cells as in a. were subjected to EdU (Green) incorporation assay (d) for 12 hours (untreated). EdU was washed away, and the cells were treated with either DMSO or the CDK4/6 inhibitor (iCDK4/6), palbociclib at 400 nM, for another 72 hours. DAPI (Blue) was used to stain nuclei. Scale bars, 50 μm. Percent of EdU⁺ nuclei were counted in at least six random fields of one representative experiment of two and plotted (e). Data plotted are mean (±SEM).f. EdU fluorescence intensity from at least six random fields from cells in d. were measured and plotted. Data plotted are mean (±SEM). (ANOVA test followed by Tukey's multiple comparisons test; Samples not sharing an alphabet are statistically significant, p < 0.01)

a corresponding reduction in the G_0/G_1 pool compared to cells with the scrambled control (Figure 1(c) and Supplemental Figure 2). To determine if the cells in S-phase could reenter the cell cycle and continue proliferating, we incubated EZH2 and scr depleted C2C12 cells with EdU for 12 hours to label as much of the cell population as possible. EdU was then removed and cells were allowed to continue proliferating, which would be indicated by a reduction in the EdU signal (Figure 1(d)). Cells were also allowed to proliferate in the presence of a CDK4/6 kinase inhibitor (iCDK4/6), palbociclib (Figure 1(d)). The percentage of EdU positive cells was quantitated (Figure 1(e)). Even after 12 hours of EdU incubation, the EZH2 depleted cells show an enhanced percentage of EdU positive cells (Figure 1(e)), consistent with our earlier data. Next, the EdU signal intensity in cells was quantitated (Figure 1(f)). We found that for both scr and EZH2 depleted cells, a significant reduction in EdU signal intensity was observed, confirming that these cells were reentering the cell cycle. Intriguingly, for EZH2 depleted cells, this reduction was blocked by iCDK4/6, indicating this effect was kinase dependent.

EZH2 represses cyclin D1 to regulate the G_1/S transition

To understand how EZH2 was promoting proliferation and regulating the G_1/S transition, we examined the expression of factors that mediate this transition, including the gene encoding cyclin D1 (*Ccnd1*). Cyclin D1 has been shown to be methylated at histone H3 lysine 27 in C2C12 cells in a PRC2 dependent manner upon differentiation [10]. We found that *Ccnd1* mRNA was upregulated (Figure 2(a)) in cells depleted for EZH2, and the upregulation of cyclin D1 was confirmed at the protein level as well (Figure 2(b)). We next examined cyclin E1 (*Ccne1*), which functions in concert with cyclin D1. We found that cyclin E1, like cyclin D1, was also upregulated at the level of mRNA (Figure 2(c)) and protein (Figure 2(d)). CDK4/6 and CDK2 are the cyclin-dependent kinases (CDK) that partner with cyclin D1 and cyclin E1, respectively. Thus, we also

examined the expression of CDK4 and CDK2 and found that they were upregulated at the mRNA level (Figure 2(e)) as well as the protein level (Figure 2(f)).

Our cell cycle analysis had shown an increase of cells in S phase and a reduction of cells in the G_2/M phase (Figure 1(c) and Supplemental Figure 2). Thus, we also examined the expression of the cyclins and cyclin dependent kinase that mediate the $S/G_2/M$ transitions. We assayed for mRNA expression of cyclin A2 (*Ccna2*) (Figure 2(g)), cyclin B1 (*Ccnb1*) (Figure 2(h)) and their partner cyclin dependent kinase, *Cdk1* (Figure 2(i)), in scr and EZH2 depleted cells and found no significant change in mRNA expression of any of these factors. As *Pax7* has shown to be repressed by PRC2, we also examined the expression of *Pax7* mRNA and found no significant change in expression (Figure 2(j)), suggesting that the depletion of EZH2 is insufficient to reactivate *Pax7* in myoblasts.

Taken together, our data strongly suggested that the effect on proliferation observed were through the upregulation of cyclin D1 and E1. To confirm that *Ccnd1* and *Ccne1* were direct targets of the PRC2 complex, we examined the EZH2 enrichment and histone modifications associated with the *Ccnd1* and *Ccne1* promoters by chromatin immunoprecipitation (ChIP) assays. To identify promoter regions that could be a target of EZH2, we examined the trimethylation of H3K27 (H3K27me3) global enrichment profile in C2C12 cells available in the WashU Epigenome browser (<https://epigenomegateway.wustl.edu/>). Primers were designed according to the methylation peaks detected in this analysis. We found that H3K27 was methylated on the *Ccnd1* promoter, and the depletion of EZH2 reduced this modification (Figure 2(k)). In cardiac cells, *Ccnd1* has been shown to be repressed by H3K9 methylation [35]. Thus, we examined the methylation of H3K9 at the *Ccnd1* promoter in cells depleted for EZH2 and found no change in the H3K9 methylation profile upon EZH2 depletion, indicating that EZH2 does not play a role in directing this modification in skeletal muscle (Figure 2(l)). We found that EZH2 was associated with the *Ccnd1*

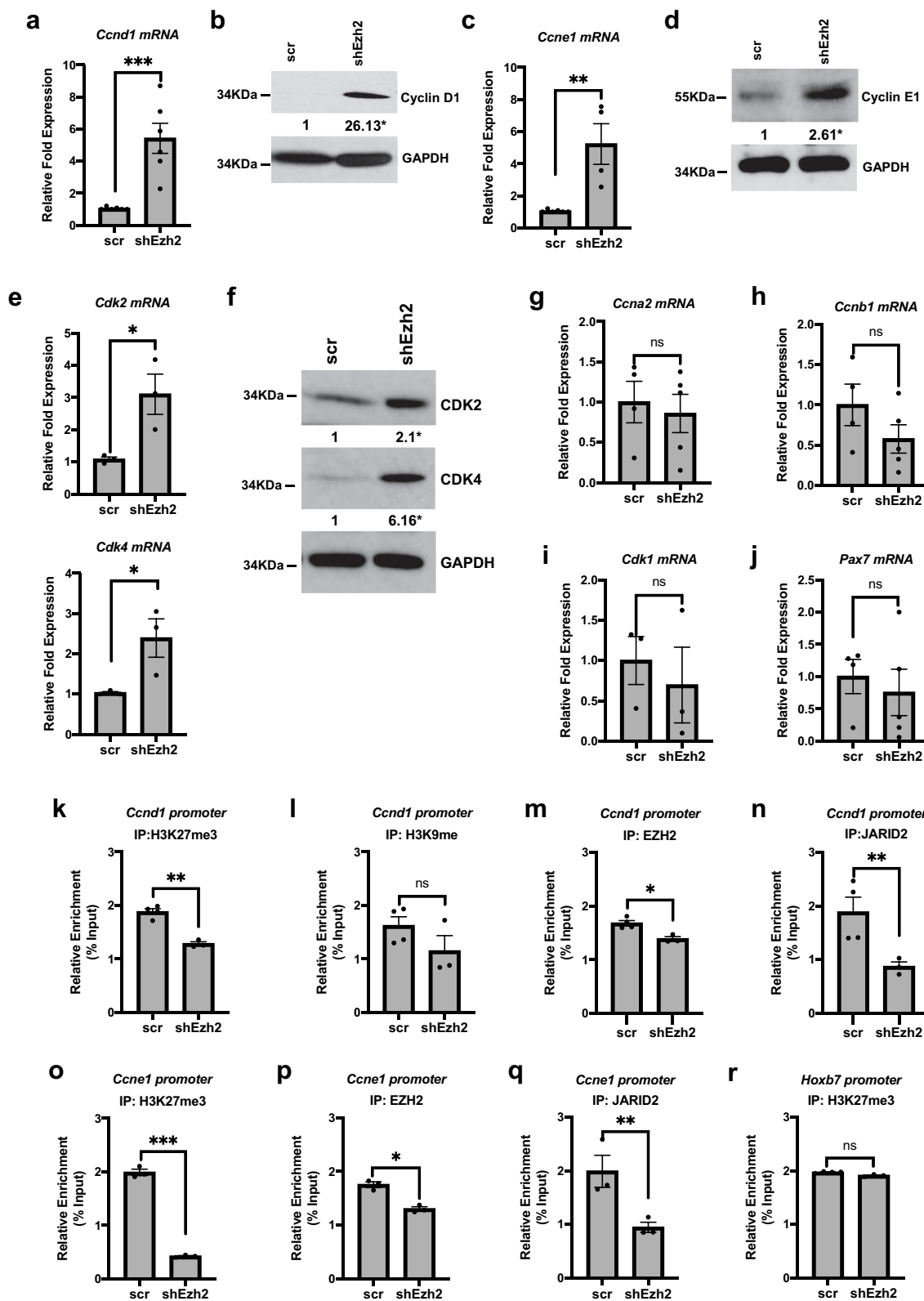


Figure 2. Pro-proliferative cell cycle genes are inhibited by EZH2.

a-b. Cyclin d1 is repressed by EZH2. Scrambled (scr) and shRNA expressing (shEzh2) C2C12 cells were assayed for cyclin d1 by qRT-PCR (a) and western blotting (b). Blots in b. were quantified, normalized to GAPDH and labeled below the blot. Data shown are mean (\pm SEM) (Student t.test, * $p < 0.05$, *** $p < 0.001$, $n = 6$ (a) & 3 (b) biological replicates).c-d. Cyclin e1 is also repressed by EZH2. Cells in a. were assayed for cyclin E1 by qRT-PCR (c) and western blotting (d). Blots in d. were quantified, normalized to GAPDH and

promoter, and this enrichment was reduced when EZH2 was depleted (Figure 2(m)). EZH2 has previously been shown to bind to the *Ccnd1* promoter in myotubes [10], but we show here that this can also be detected in myoblasts. We also asked if JARID2 was associated with the *Ccnd1* promoter. We found that JARID2 was bound to the promoter and this enrichment was diminished upon EZH2 depletion (Figure 2(n)).

We next asked if *Ccne1* was also a direct target of the PRC2 complex. We found that H3K27 methylation could be detected at the *Ccne1* promoter, and this enrichment was reduced upon EZH2 depletion (Figure 2(o)). EZH2 was found to be associated with the *Ccne1* promoter, and EZH2 depletion reduced this association (Figure 2(p)). We also found that JARID2 was recruited to the *Ccne1* promoter and this recruitment was dependent on the presence of EZH2 (Figure 2(q)). As a positive control for our ChIP experiments, we also examined the enrichment of H3K27me3 at the *Hoxb7* promoter (Figure 2(r)), a well-characterized target of PRC2 [36]. To compare enrichments on the *Hoxb7* and *Ccnd1* promoters, we also plotted the data as percent input (Supplemental Figure 3). By this analysis, it can be seen that H3K27me3 is more enriched at the *Hoxb7* locus. However, the depletion of EZH2 did not reduce H3K27me3 at the *Hoxb7* promoter, indicating that the methylation of *Ccnd1* is a more dynamic modification.

Cyclin D1 regulates the cell cycle by inhibiting the function of pRB (*Rb1*) through direct phosphorylation [37]. RB1 is required for the irreversible cell

cycle exit associated with the arrest of myoblasts and myogenic differentiation [9,10]. Thus, we examined the protein expression of RB1 and found that RB1 expression was inhibited when EZH2 was depleted (Figure 3(a)). We also examined the phosphorylation of RB1 and found that RB1 was heavily phosphorylated in EZH2 depleted cells. Our results show that RB1 is strongly inhibited both by phosphorylation and overall expression in EZH2 depleted cells where cyclin D1 is upregulated. The phosphorylation of RB1 also confirms that cyclin D1 and associated cyclin dependent kinases are active in these cells (Figure 3(a)).

To understand if the inhibition of RB1 was directly mediated by the PRC2 complex or a result of cyclin D1 overexpression, we examined the *Rb1* promoter for the presence of EZH2. We found that EZH2 was associated with the *Rb1* promoter (Figure 3(b)). Correspondingly, we also found that H3K27me3 was enriched on the *Rb1* promoter, and this enrichment was decreased upon EZH2 depletion (Figure 3(c)). We also examined the methylation of H3K9 but observed no change in the enrichment upon the depletion of EZH2 (Figure 3(d)). The presence of JARID2 was also examined, and we found that JARID2 was associated with the *Rb1* promoter in an EZH2 dependent manner (Figure 3(e)). Thus, *Rb1* is a direct target of the PRC2 complex. However, our data clearly show that relieving PRC2 mediated inhibition is not sufficient to activate *Rb1* in the presence of cyclin D1

We also examined the expression of p21 (*Cdkn1a*), which is also required for cell cycle

labeled below. Data shown are mean (\pm SEM) (Student t.test, *p < 0.05, **p < 0.01, n = 4(c) and 3(d) biological replicates)E-f. Cyclin-dependent kinases (Cdk) are upregulated upon EZH2 depletion. Cells as in a. were assayed for mRNA levels of *Cdk2* and *Cdk4* by qRT-PCR (e) and protein by western blot assays (f). Blots in f. were normalized to GAPDH and labeled below the blot. Data shown are mean (\pm SEM) (Student t.test, *p < 0.05, n = 3 biological replicates).g-l. Cyclin A2 (*Ccna2*), Cyclin B1 (*Ccnb1*) and *Cdk1* are unaltered upon EZH2 depletion. Cells as in a. were assayed for mRNA levels of *Ccna2* (g), *Ccnb1* (h) and *Cdk1* (l) by qRT-PCR. Data shown are mean (\pm SEM) (Student t.test, ns represents "not significant", n = 3–5 biological replicates).j. *Pax7* is not upregulated upon EZH2 depletion. Cells as in a. were assayed for mRNA levels of *Pax7* by qRT-PCR. Data shown are mean (\pm SEM) (Student t.test, ns represents "not significant", n = 3–5 biological replicates).K-n. Cyclin D1 (*Ccnd1*) is directly repressed by the PRC2 complex. ChIP assays for H3K27me3 (k), H3K9me (l), EZH2 (m) and JARID2 (n) enrichment on *Ccnd1* promoter in cells as in a. Igg background signals were subtracted from IP signals. Data shown are mean (\pm SEM) (Student t.test, ns represents "not significant", *p < 0.05, **p < 0.01, n = 3–4 biological replicates).o-r. Cyclin e1 is also directly repressed by the PRC2 complex. ChIP assay for H3K27me3 (o), EZH2 (p) and JARID2 (q) enrichment on the *Ccne1* promoter in cells as in a. Primers spanning *Hoxb7* locus (R) was used as a positive control for H3K27me3 enrichment. Igg background signals were subtracted from IP signals. Data shown are mean (\pm SEM) (Student t.test, ns represents "not significant", *p < 0.05, **p < 0.01, ***p < 0.001, n = 3 biological replicates).

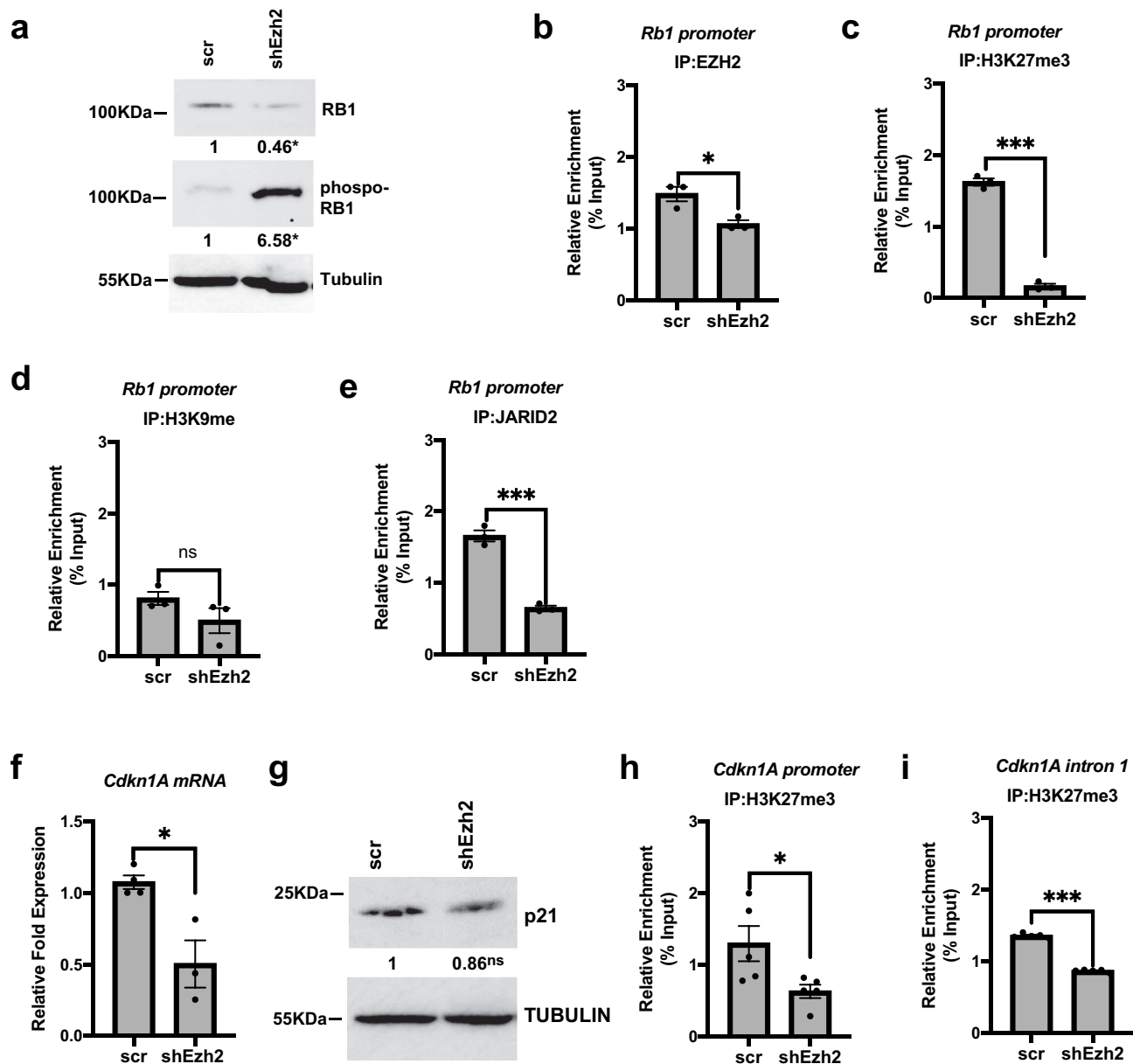


Figure 3. Negative cell cycle regulators are also directly regulated by the PRC2 complex.

a. RB1 is inhibited in EZH2 depleted cells. Proliferating, asynchronous scrambled (scr) and EZH2 depleted (shEzh2) C2C12 cells were assayed by western blot assays (a). Blot was quantified, normalized, and labeled below the blot. Data shown are mean (\pm SEM) (Student t-test, * $p < 0.05$, $n = 3$ biological replicates). b-e. *Rb1* is directly regulated by the PRC2 complex. ChIP assays were performed on cells as in a. with antibodies against EZH2 (b), H3K27me3 (c), H3K9me and JARID2 (e) and primers spanning the *Rb1* promoter. IgG background signals were subtracted from IP signals. Data shown are mean (\pm SEM) (Student t-test, ns represents "not significant", * $p < 0.05$, *** $p < 0.001$, $n = 3$ biological replicates). f-g. *Cdkn1a* mRNA is downregulated upon EZH2 depletion. Cells in a. were assayed for p21 at mRNA level (f) and protein level (g) by qRT-PCR and western blotting, respectively. Blots in g. were normalized to Tubulin, and labeled below the blot. Data shown are mean (\pm SEM) (Student t-test, ns represents "not significant", * $p < 0.05$, $n = 3$ biological replicates). h-i. ChIP assays were performed on cells as in a. with antibodies against H3K27me3 and primers spanning the *Cdkn1a* promoter (h) and intron 1 (i). IgG background signals were subtracted from IP signals. Data shown are mean (\pm SEM) (Student t-test; * p -value < 0.05 , *** $p < 0.001$, $n = 3-5$ biological replicates).

exit. We found that *Cdkn1a* mRNA expression was modestly inhibited upon EZH2 depletion (Figure 3 (f)). We also examined the protein expression of

p21 and found that the expression was relatively unchanged (Figure 3(g)). Importantly, neither the mRNA or protein analysis of p21 showed an

upregulation of p21 and instead, suggested a modest inhibition of p21 that would be expected in proliferating cells. To determine if *Cdkn1a* was a direct target of the PRC2 complex, we examined the histone methylation of two previously identified regions of the *Cdkn1a* promoter associated with H3K27me3. The depletion of EZH2 reduced the H3K27me3 detected at both the *Cdkn1a* promoter (Figure 3(h)) and the first intron region (Figure 3(i)). Thus, our data show that *Cdkn1a* is a direct target of the PRC2 complex. However, like *Rb1*, the loss of H3K27me3 is not sufficient to activate *Cdkn1a* in the presence of cyclin D1.

These results were highly surprising given that the PRC2 complex has been shown to be required for cell viability in multiple systems, including skeletal muscle. To rectify our findings with previous work, we transiently depleted EZH2 in C2C12 cells, similar to the approach used to show that EZH2 was required for viability in human cells [34]. We utilized this approach in a previous study, where we showed that transient depletion of EZH2 in C2C12 cells led to an upregulation of *Myog* [30], as has been observed by other studies [36,38–40]. Here, we used the same approach to examine proliferation and *Ccnd1* expression. C2C12 cells were transiently transfected with the shRNA constructs used for the stable cell line generation. In this approach, we observed no enhancement of proliferation and instead, a slight decrease in proliferation (Figure 4(a)). Down-regulation of EZH2 was confirmed by mRNA and protein expression (Figure 4(b)). To correlate this with our previous findings, we examined the expression of *Ccnd1* and found that *Ccnd1* mRNA was upregulated 24 hours after transfection, but the levels quickly returned to baseline 48 hours after transfection (Figure 4(c)). As a control for our assay, we assayed *myogenin* mRNA expression, which has been previously shown to be directly regulated by the PRC2 complex [36]. Like *Ccnd1*, we observed a transient upregulation of *Myog* by 24 hours post transfection (Figure 4(d)). The protein expression of cyclin D1 was also examined at 24 and 48 hours post-transfection and no upregulation of cyclin D1 could be seen at either time point (Figure 4(e)).

We also examined mRNA levels of *Ccna2* (Figure 4(f)), *Ccnb1* (Figure 4(g)) and *Cdk1* (Figure 4(h)) and found a modest elevation in the expression of each of these factors required for the S/G2/M transition, consistent with the mild decrease in proliferation observed in the cells.

Together these results confirm that our experimental approach could recapitulate what has been previously reported, but highlight the profound differences obtained from a transient versus stable depletion of EZH2. To understand the mechanistic basis for this effect, we turned to primary myoblast cells. C2C12 cells are known to have a deletion in the *Ink4a* locus that prevents expression of *P19ARF*. Thus, in C2C12 cells, suppression of *Rb1* is sufficient to induce S phase reentry [41]. Given that we showed that RB1 was inactivated in EZH2 depleted cells, it was unclear if the absence of *P19ARF* in C2C12 cells was contributing to the cell cycle effects observed.

EZH2 is required for viability but promotes proliferation in primary myoblasts

To understand the effect of EZH2 depletion in primary myoblasts, we transiently transfected shEZH2 into freshly isolated primary myoblasts and assessed cell proliferation. Consistent with prior studies, we found that the depletion of EZH2 led to a sharp decrease in cell proliferation (Figure 5(a)). The depletion of EZH2 was confirmed at the level of mRNA (Figure 5(b)) and protein (Figure 5(c)). The cell cycle profile was analyzed by flow cytometry. We found that many of the cells were non-viable upon EZH2 depletion, again consistent with prior work. However, surprisingly, in the viable cell population, EZH2 depleted cells were more highly enriched in S phase (Figure 5(d) and Supplemental Figure 4). To confirm this result, primary myoblasts transiently depleted for EZH2 were also examined for EZH2 expression and EdU incorporation by immunofluorescence. We found that the overall level of EZH2 was reduced in the EZH2 depleted cells and that an increase in EdU positive cells could be observed (Figure 5(e)). These results strongly suggested that the depletion of EZH2

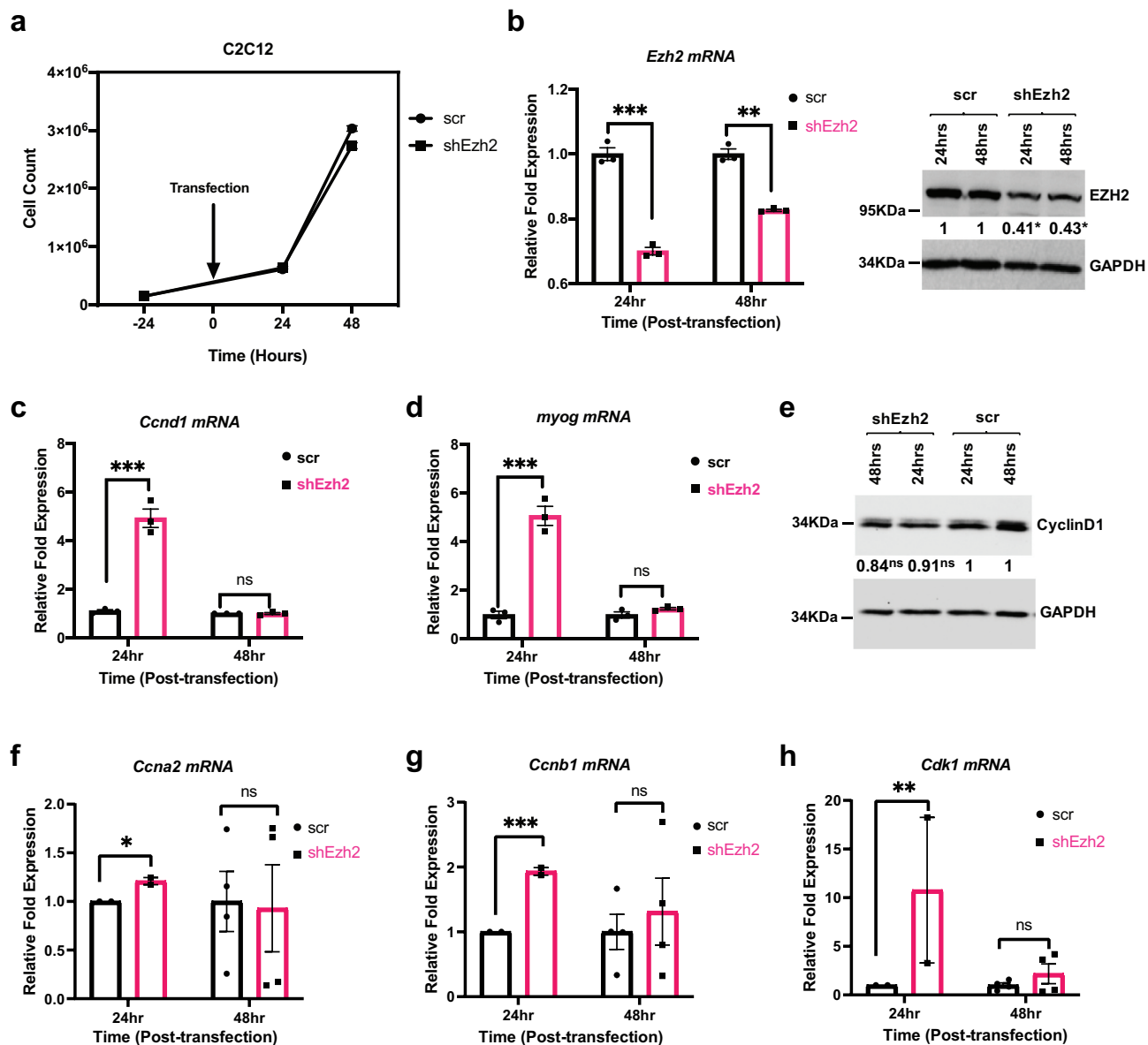


Figure 4. Transient transfection of shEzh2 in C2C12 mildly decreases cell proliferation.

a. Cell proliferation assay in C2C12 cells either transfected with scrambled control (scr) or shRNA against EZH2 (shEzh2) as indicated. Data plotted are mean (\pm SEM) ($n = 3$ biological replicates). b. Confirmation of EZH2 depletion in C2C12 cells in a. by qRT-PCR (left) and western blot (right). Data plotted are mean (\pm SEM) (Student t.test, $^{**}p < 0.01$, $^{***}p < 0.001$, $n = 3$ biological replicates). c-d. *Ccnd1* (c) and *Myog* (d) are transiently upregulated upon transient loss of EZH2 in C2C12 cells. Cells in a. were assayed for mRNA expression by qRT-PCR. Data plotted are mean (\pm SEM) (Student t.test, ns represents "not significant", $^{***}p < 0.001$, $n = 3$ biological replicates). e. Cells in a. were assayed at the protein level for cyclin d1 by western blot. The blots were quantified, normalized to GAPDH and labeled below the blot (Student t.test, $^{*}p < 0.05$, $n = 3$ biological replicates). f-h. *Ccna2* (f), *Ccnb1* (g) and *Cdk1* (h) are transiently upregulated upon transient loss of EZH2 in C2C12 cells. Cells in A. were assayed for mRNA expression by qRT-PCR. Data plotted are mean (\pm SEM) (Student t.test, ns represents "not significant", $^{*}p < 0.05$, $^{**}p < 0.01$, $^{***}p < 0.001$, $n = 3$ biological replicates).

could either promote cell death or enhance proliferation. To confirm this potential dual effect, we examined the expression of cleaved caspase-3 to detect apoptotic cells and EdU to detect

proliferation in EZH2 depleted cells. We found both an increase in the EdU positive population and the cleaved caspase-3 positive cell population upon EZH2 depletion (Figure 5(F) and

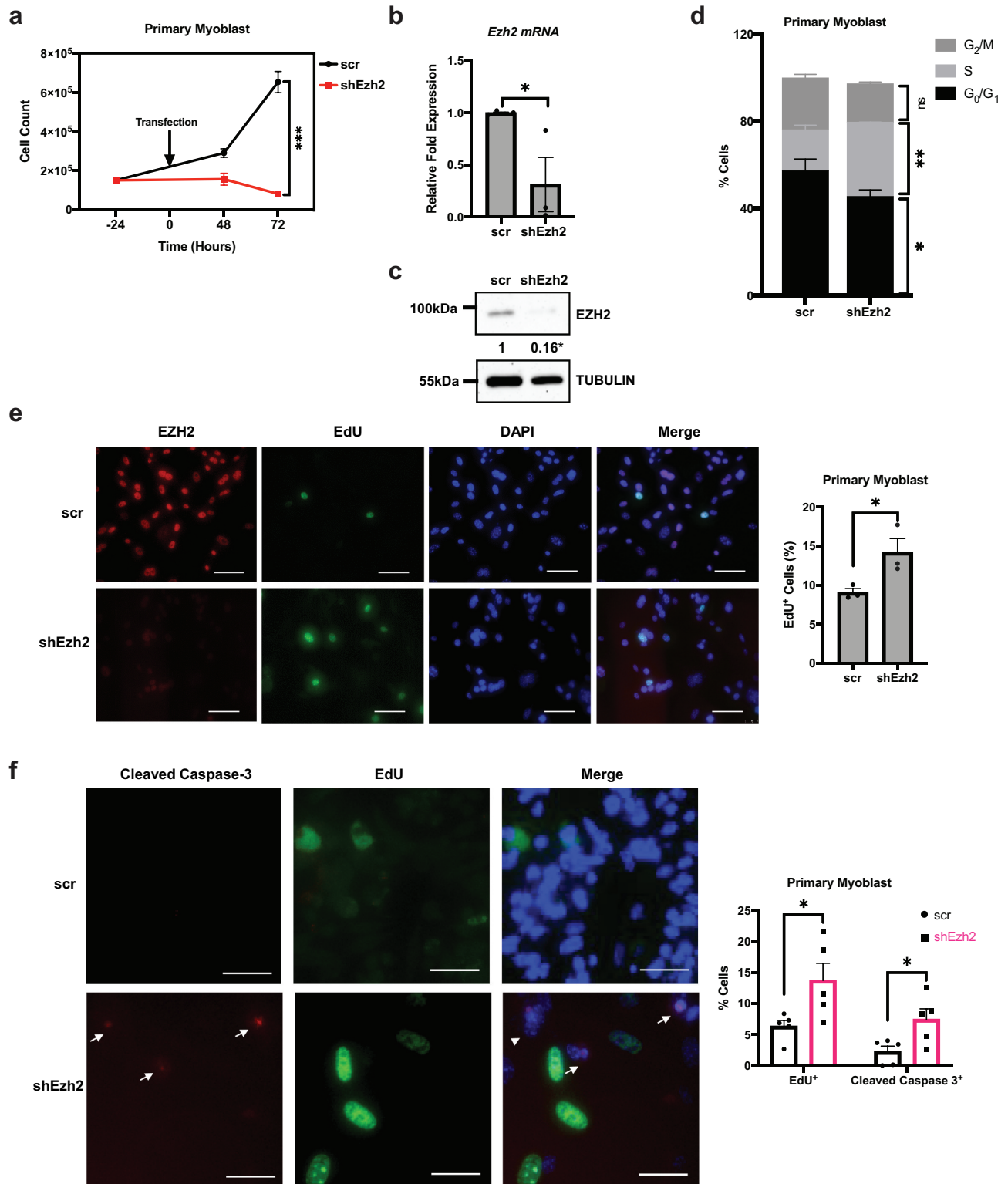


Figure 5. Transient loss of EZH2 in primary myoblasts decreases cell viability and also has increased proliferative cell population. a. Transient loss of EZH2 in primary myoblasts shows decreased cell viability. Cell proliferation assay in primary myoblast cells either transfected with scrambled control (scr) or shRNA against EZH2 (shEzh2) as indicated. Data plotted are mean (\pm SEM) (Student t.test, *** $p < 0.001$, $n = 3$ biological replicates). B-c. EZH2 depletion in primary myoblasts was confirmed by qRT-PCR (b.) and wesyrn blot (c.). Blots in c. were normalized to Tubulin, and labeled below the blot. Data plotted are mean (\pm SEM) (Student t.test, * $p < 0.05$, $n = 3$ biological replicates). d. Increased s-phase cell population among viable cells upon transient EZH2 depletion. Primary myoblasts in

Supplemental Figure 5). We found that EZH2 depleted cells were either EdU positive or cleaved caspase-3 positive, indicating that cells either initiated apoptosis or increased DNA synthesis. These results strongly suggested that there were two distinct cell populations, likely correlated with the level of EZH2 depletion.

We next examined gene expression in the primary myoblasts transiently depleted for EZH2, and found that the results largely confirmed what we found with a transient approach in C2C12 cells. In primary myoblasts transiently depleted for EZH2, both *Myog* (Figure 6(a)) and *Myod1* (Figure 6(b)) were upregulated upon transient EZH2 depletion. Consistent with the high degree of non-proliferative cells observed in this approach (Figure 5(a)), we found that *Ccnd1* (Figure 6(c)) and *Ccne1* (Figure 6(d)) were downregulated, as were *Cdk2* (Figure 6(e)) and *Cdk4* (Figure 6(f)). We found that *Cdkn1a* (p21) was upregulated (Figure 6(g)). *Cdkn2a* (corresponding to both *p19^{ARF}* and *p16^{INK4A}*) was downregulated (Figure 6(h)), suggesting that the loss of this locus in C2C12 cells likely did not contribute to our earlier results. We also examined *Ccna1* and *Ccnb1* expression and found that both cyclins were modestly upregulated (Figure 6(i,j)). *Pax7* mRNA expression was unaffected (Figure 6(k)). The downregulation of cyclin D1 and associated cyclin dependent kinases and a modest upregulation of p21 were confirmed by western blot analysis (Figure 6(l)). We also examined two markers of apoptosis, *Bax* and *Bcl2*. *Bax* is considered a pro-apoptotic marker, while *Bcl2* is an anti-apoptotic marker. We found that *Bax* mRNA was upregulated (Figure 6(m)), while *Bcl2* mRNA was not significantly changed (Figure 6(n)).

Together, these results showed that transient depletion of EZH2 in primary myoblasts leads to upregulation of negative cell cycle genes, such as p21, suppression of positive cell cycle genes, and an upregulation of the pro-apoptotic *Bax* gene. The cyclins responsible for the G1/S transition, cyclin D and cyclin E, were downregulated, while the cyclins for the S/G2/M transition, cyclin A and cyclin B, were upregulated.

Our results suggested that there were two populations of cells upon EZH2 depletion; one which promoted entry into S phase and enhanced proliferation and one which exited the cell cycle and initiated apoptosis. We hypothesized that the level of EZH2 in cells might underlie this difference. Cells with modestly reduced EZH2 would upregulate *Ccnd1* and proliferate, while severe EZH2 depletion would inhibit proliferation and result in cell death. To test this hypothesis, we used a chemical inhibitor of EZH2, GSK126 [42]. Primary myoblasts were treated with varying concentrations of GSK126, and we found that low concentrations indeed enhanced proliferation, while higher concentrations inhibited cell growth (Supplemental Figure 6). Enhanced proliferation in the presence of a low concentration of GSK126 is also shown in Figure 7(a). To correlate these changes with the gene expression results we had seen, primary myoblasts were treated with low concentrations of GSK126 and harvested for RNA analysis (Figure 7(b)). Consistent with our initial results from the stable, modest depletion of EZH2 in C2C12 cells, we found that *Ccnd1* and *Ccne1* were upregulated, as were *Cdk2* and *Cdk4*. Intriguingly, *Rb1* was also upregulated in this approach while *Cdkn1a* was downregulated. Proliferating cell nuclear antigen (*Pcna*), which is

A. were sorted at 48 hours post-transfection of scrambled control (scr) or shEzh2 using flow cytometer after propidium iodide staining and analyzed using FlowJo software (Fig. S5). Data plotted are mean (\pm SEM) (Student t.test, ns represents "not significant", * $p < 0.05$, ** $p < 0.01$, $n = 2$ biological replicates). E. EZH2 depletion has increased DNA synthesis. Primary myoblasts as in a. were subjected to EdU incorporation assay. EdU (Green) and EZH2 (Red) were stained. DAPI (Blue) was used to stain the nuclei (e, left panel). Scale bars, 100 μ m. Percent of EdU⁺ nuclei were counted in at least ten random fields and plotted (right panel). Data plotted are mean (\pm SEM) (Student t.test, * $p < 0.05$, $n = 3$ biological replicates). f. Both proliferative and apoptotic cell populations increase on EZH2 loss in primary myoblast cells. Cells as in a. were subjected to EdU (Green) incorporation assay. Cleaved Caspase-3 (Red, Arrowhead) was stained for apoptotic cells. DAPI (Blue) was used to stain nuclei. Scale bars, 100 μ m. Percent of EdU⁺ and Cleaved-Caspase 3⁺ nuclei were counted in at least five random fields and plotted (right panel). Data plotted are mean (\pm SEM) (Student t.test, * $p < 0.05$, $n = 2$ biological replicates).

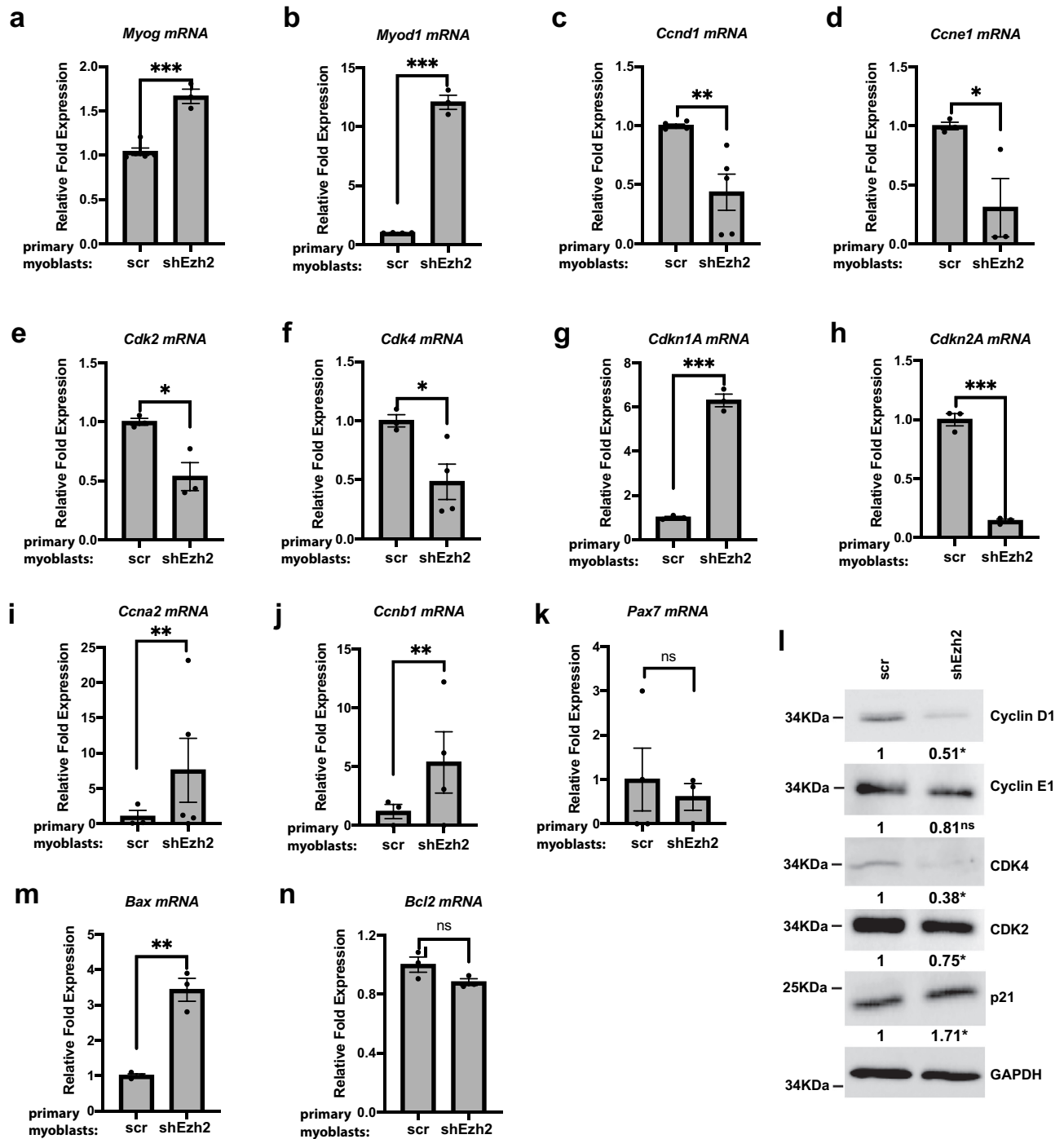


Figure 6. Transient loss of EZH2 in primary myoblasts leads to increased MRF and negative cell cycle gene expression while positive cell cycle genes are downregulated.

a-b. *Myog* and *Myod1* expression are upregulated upon loss of EZH2 in primary myoblasts. Primary myoblast cells transiently transfected with scramble control (scr) or shEzh2, 48 hours post-transfection, were assayed for mRNA expression of *Myog* (a) and *Myod1* (b) by qRT-PCR. Data plotted are mean (\pm SEM) (Student t.test, *** $p < 0.001$, $n = 3$ biological replicates). c-j. Cell cycle genes are deregulated upon loss of EZH2. Cells in a. were assayed for mRNA expression of *Ccnd1* (c), *Ccne1* (d), *Cdk2* (e), *Cdk4* (f), *Cdkn1a* (g), *Cdkn2a* (h), *Ccna2* (i) and *Ccnb1* (j), by qRT-PCR. Data plotted are mean (\pm SEM) (Student t.test, * $p < 0.05$, ** $p < 0.01$, *** $p < 0.001$, $n = 3-5$ biological replicates). k. PAX7 is not upregulated upon depletion of EZH2 in primary myoblasts. Cells in A were assayed for mRNA expression by qRT-PCR. Data plotted are mean (\pm SEM) (Student t.test, ns represents "not significant", $n = 3-5$ biological replicates). l. Western blot analysis of cells in a. for cyclin D1, cyclin E1, CDK4, CDK2 and p21. GAPDH was used as a loading control. A representative blot of three biological replicate experiments is shown. Blots in l. were quantified, normalized to

required for DNA replication and a marker for S phase, was also highly upregulated. Importantly, we found that the mRNA expression of *p16^{INK4a}* and *p19^{ARF}* were unchanged, suggesting again that the absence of this locus does not underlie the effects on proliferation we observed in C2C12 cells. We also examined the protein expression of cell cycle factors in the presence of low concentrations of GSK126 and found that the upregulation of cyclin D1, CDK4 and CDK2 could be observed at the protein level (Figure 7(c)). We also saw an upregulation of RB1, but the change in p21 was not significant (Figure 7(c)). As a control for the study, we also examined MYOG, a well characterized target of the PRC2 complex and found, as anticipated, that it was upregulated (Figure 7(c)).

This experiment was repeated in C2C12 cells and we found similar results, although the absolute concentrations of the drugs required to see the effects differed between the cell lines (Supplemental Figure 6). For C2C12 cells, a low concentration of GSK126 again enhanced cell proliferation (Figure 8(a)). mRNA expression analysis showed an upregulation of *Ccnd1*, *Ccne1*, *Cdk2* and *Cdk4* (Figure 8(b)). *Pcna* was also upregulated. We found that *Rb1* was upregulated while *Cdkn1A* was unchanged in expression, as were *Myog* and *MyoD1*. Cyclin D1 and CDK4 expression were also examined at the protein level, and we found that cyclin D1 and CDK4 were indeed upregulated upon modest inhibition of EZH2 (Figure 8(c)). Finally, we performed a ChIP analysis for H3K37me3 enrichment in C2C12 cells exposed to a low concentration of GSK126. We found that reductions in H3K27me3 enrichment were observed on the *Ccnd1*, *Ccne1*, *Myog*, *Rb1* and *Cdkn1a* promoters (Figure 8(d)), consistent with the ChIP results shown for the modest, stable depletion of EZH2 in C2C12 cells and confirmation that the low dose of GSK126 did inhibit EZH2 activity.

Discussion

In this work, we show that the PRC2 complex has the unexpected function to restrain proliferation by repressing the pro-proliferative cell cycle regulators, *Ccnd1* and *Ccne1*, in skeletal muscle. Intriguingly, the PRC2 complex also represses negative cell cycle genes such as *Rb1* and *Cdkn1a*, the repression of which prevents mitotic exit and terminal differentiation. Thus, the normal function of the PRC2 complex in skeletal muscle appears to be restraining the rate of proliferation while also preventing mitotic exit by directly repressing both positive and negative cell cycle regulators as summarized in Figure 8(e). Our work shows that positive cell cycle regulators appear to be more sensitive to PRC2 repression compared to negative regulators, suggesting that cells may have a certain threshold level of EZH2 that is maintained during myoblast proliferation until they receive a cue for cell cycle exit and differentiation.

It is interesting that the PRC2 complex directly regulates both cyclin D1 and cyclin E1 to maintain control of the cell cycle. The dual regulation serves to maintain control of two central regulators of S phase. Our results suggest that the PRC2 complex has many divergent roles in skeletal muscle cells that requires a fine balance of EZH2 expression throughout the progression of proliferation and differentiation. In the stable C2C12 EZH2 depletion cell line characterized here, the loss of inhibition of cyclin D1 clearly dominates the potential derepression of *Rb1*. This effect was not observed in the time course of treatment with low concentrations of GSK126, where both *Ccnd1* and *Rb1* were upregulated, which suggests that it is the sustained modest depletion of EZH2 that leads to the upregulation of *Ccnd1* and the cyclin D1 dependent repression of *Rb1*.

The PRC2 complex plays many roles in mediating the cell fate transitions that occur during

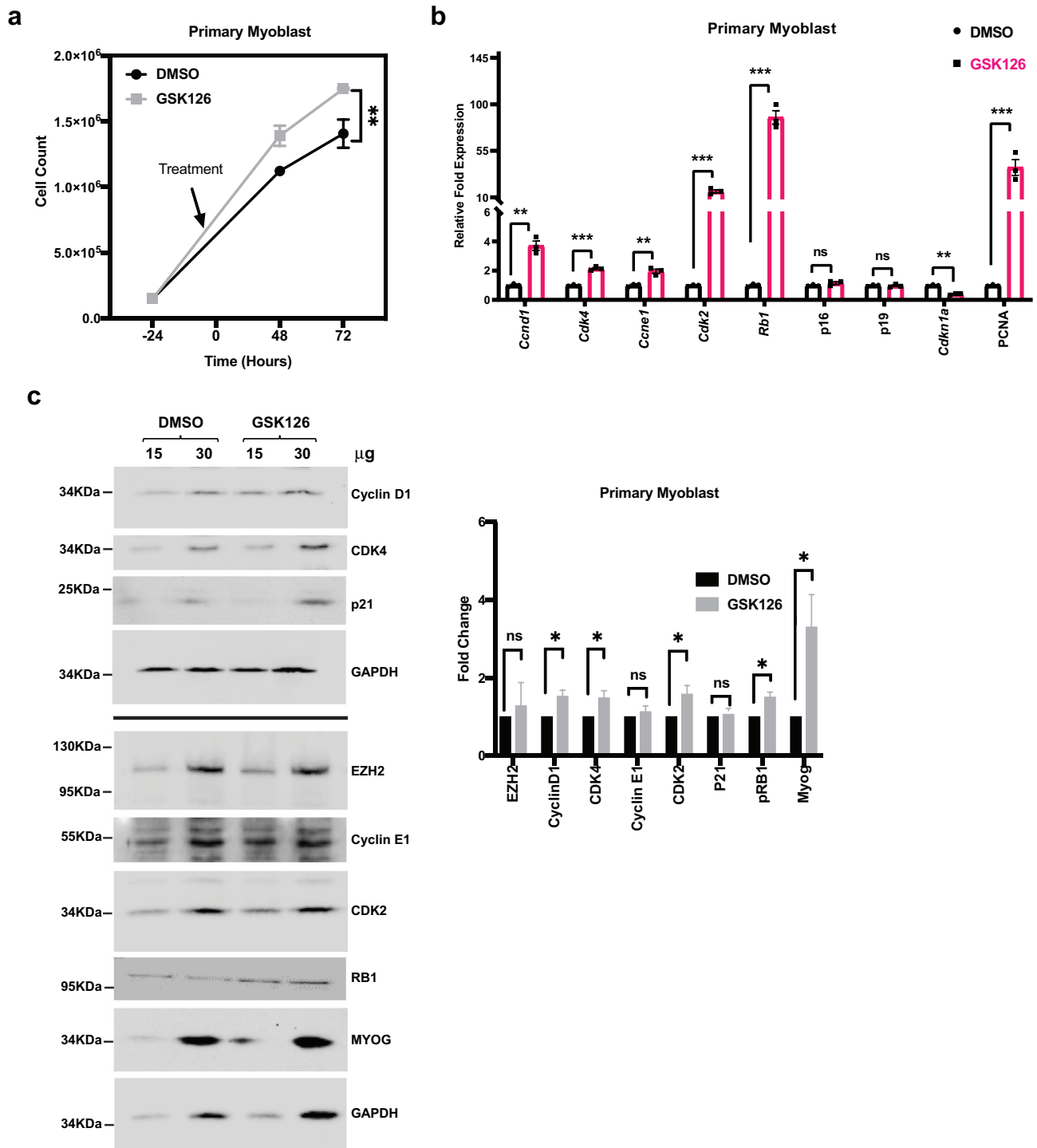


Figure 7. Catalytic inhibition of EZH2 by GSK126 at low concentrations enhances proliferation in primary myoblasts.

a. Cell proliferation curve of primary myoblast cells upon treatment with 0.03% DMSO control and 0.66 μM EZH2 inhibitor, GSK126. Data plotted are mean (\pm SEM) (Student t.test, ** $p < 0.001$, $n = 4$ biological replicates). b. Cell cycle genes are deregulated on inhibition of EZH2 activity by GSK126. Primary myoblast cells as in A. were treated with DMSO control and 0.66 μM GSK126 for 72 hours. mRNA expression of cell cycle genes and myogenic regulatory factors (MRFs) were assayed by qRT-PCR. Data plotted are mean (\pm SEM) (Student t.test, ns represents "not significant", ** $p < 0.01$, *** $p < 0.001$, $n = 3$ biological replicates). c. The protein level of cell cycle gene expression was assayed in primary myoblast cells treated with DMSO control and GSK126 (left panel). The samples were loaded at 15 and 30 μg protein concentration. Blots in C. were quantified, normalized to GAPDH and plotted (right panel). Data shown are mean (\pm SEM) (Student t.test, ns represents "not-significant", * $p < 0.05$, $n = 3$ biological replicates).

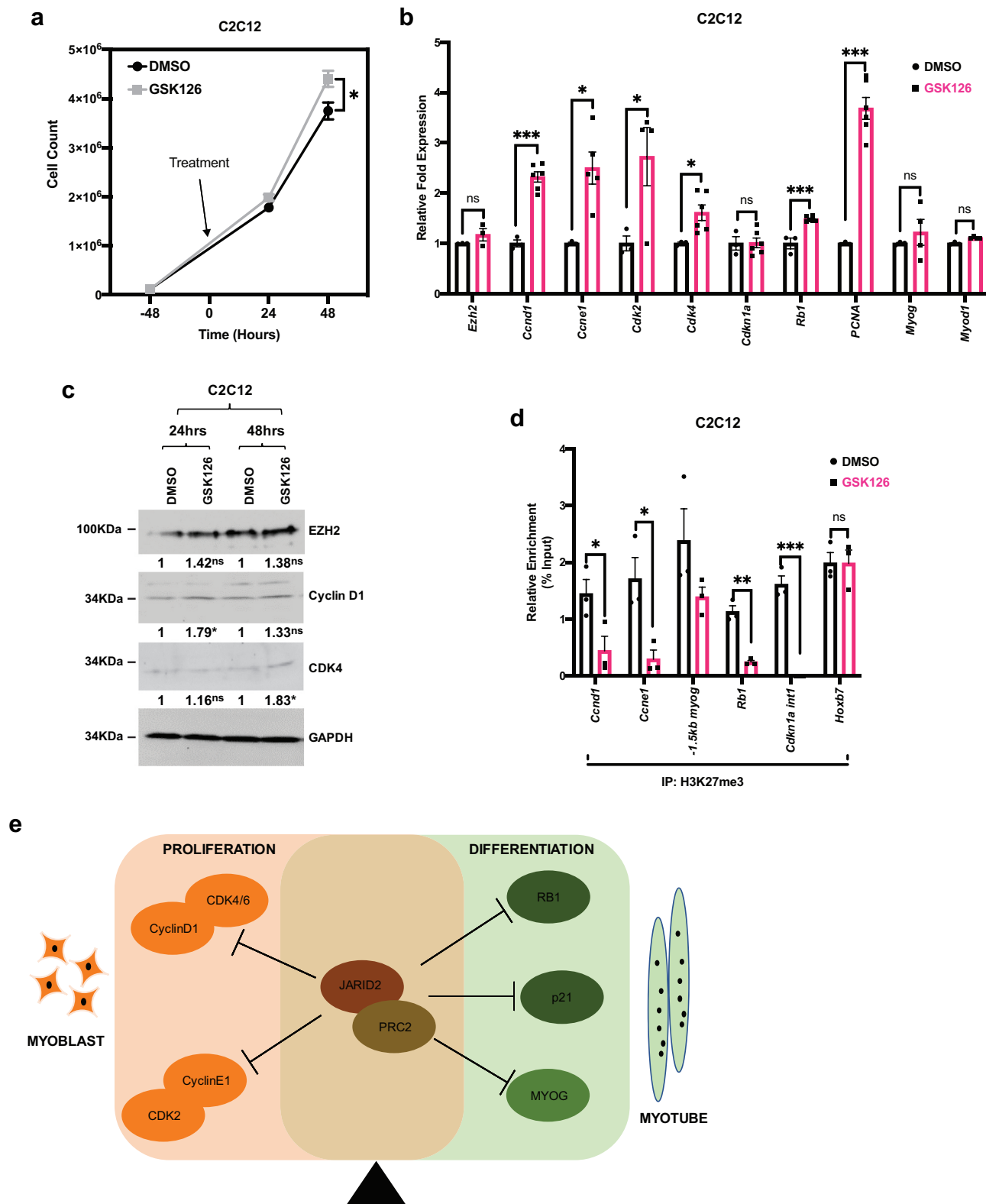


Figure 8. EZH2 inhibition by low concentration of GSK126 in C2C12 cells recapitulates increased cell proliferation.

A. Cell proliferation curve of C2C12 cells upon treatment with 0.06% DMSO control and 1.25 μ M EZH2 inhibitor, GSK126. Data plotted are mean (\pm SEM) (Student t.test, * $p < 0.05$, $n = 3$ biological replicates). B. Cell cycle genes are deregulated on inhibition of EZH2 activity by GSK126. C2C12 cells as in A. were treated with DMSO control and 1.25 μ M GSK126 for 48 hours. mRNA expression of various cell cycle genes, myogenic regulatory factors (MRFs) were assayed by qRT-PCR. Data plotted are mean (\pm SEM) (Student t.test,

myogenesis. While the inflammatory signaling mediated repression of *Pax7* was known to occur only in MSCs, *Pax7* was known to be constitutively repressed by PRC2 in myotubes [24]. Our results show that depletion of EZH2 is insufficient to derepress *Pax7* in committed myoblasts. It is highly likely that additional repression mechanisms function to maintain *Pax7* silencing in myotubes.

Polycomb group proteins are antagonistic to the Trithorax group of proteins and the balance between these complexes is thought to govern normal gene regulation, with perturbations to this balance leading to pathogenesis and disease [43]. PRC2 also localizes to replication forks and loss of function affects the progression of DNA replication forks [44]. Consistent with other data supporting a role for EZH2 in proliferation [19,34], we found that transient expression of shEZH2 did lead to reductions in cell viability. However, the cells that were viable showed accumulations in S phase. Modest chemical inhibition of EZH2 also led to enhanced proliferation, while severe chemical inhibition leads to growth reduction and cell death. It is worth noting that we used five individual shRNA constructs against EZH2 to generate the stable EZH2 depletion cell lines and all constructs generated either no or modest depletions. Characterization of the modest EZH2 depletion cell lines we recovered showed enhanced proliferation and stable enhanced expression of cyclin D1. In this work, we identified two individual shRNA constructs that resulted in significant EZH2 depletion so we also generated stable cell lines with pooled shRNA constructs but found no additional depletion of EZH2. These data strongly suggest that cells can only tolerate a modest

depletion of EZH2 and that more significant depletions of EZH2 result in a loss of viability.

Our data support a model where the PRC2 complex acts to tightly control cellular growth by repressing both positive and negative cell cycle regulators, yet also maintains other critical functions in the cell. The loss of EZH2 triggers cell death, and the upregulation of positive cell cycle regulators such as cyclin D1 and cyclin E1 are quickly lost. The results with *Rb1* are intriguing. It has been shown that inhibition of *Rb1* is sufficient to induce S phase reentry in C2C12 cells, but primary myoblasts require suppression of both *Rb1* and *P19ARF* for S phase reentry [41]. In our study, modest inhibition of EZH2 induced S phase reentry by upregulating *Ccnd1*, irrespective of the upregulation of *Rb1*. *P19ARF* locus expression was unchanged, indicating that suppression of the locus is not required for S phase reentry with the EZH2 dependent upregulation of *Ccnd1* and *Ccne1*.

It is interesting that the MRFs are known to regulate several genes critical for cell cycle progression [45] and the PRC2 complex controls both MRF expression and the cell cycle machinery. This interplay profoundly regulates the fate of a myogenic cell by controlling the decision to proliferate or exit the cell cycle to initiate differentiation.

EZH2 has been implicated as both an oncogene and a tumor suppressor in cancer [46], and our results support how EZH2 could promote or suppress proliferation depending on the overall levels and co-factors present in the cell. Our results show that loss of H3K27me3 on a promoter is not sufficient for the expression of a given gene, and it is likely the cellular context and the other transcription factors available

ns represents "not significant", * $p < 0.05$, *** $p < 0.001$, $n = 3$ biological replicates).C. Expression of EZH2, cyclin D1 and CDK4 were assayed at the protein level by western blot after 24 and 48 hours of DMSO and GSK126 treatment. GAPDH was used as loading control. Blots in C. were quantified, normalized to GAPDH and labeled below the blots. Data shown are mean. (Student t.test, ns represents 'not significant', * $p < 0.05$, $n = 3$ biological replicates).D. H3K27me3 is reduced on cell cycle genes in C2C12 cells treated with the EZH2 inhibitor, GSK126. ChIP assays for H3K27me3 enrichment on the promoters of cyclin D1 (*Ccnd1*), cyclin E1 (*Ccne1*), myogenin (*Myog*), *Rb1* and intron 1 of p21 (*Cdkn1a*) in C2C12 cells treated with 0.06% DMSO control and 1.25 μ M GSK126 cells for 48 hours. IgG background signals were subtracted from IP signals. IP signals below background was zeroed. Data plotted are mean (\pm SEM) (Student t.test, * $p < 0.05$, ** $p < 0.01$, *** $p < 0.001$, $n = 3$ biological replicates).E. A schematic model showing the regulation of both positive and negative regulators of the cell cycle by the PRC2 complex to balance skeletal muscle proliferation and differentiation.

govern which genes are expressed. Both *Myog* and *Rb1* are examples of this. While both are targets of EZH2 and show immediate upregulation upon depletion or inhibition of EZH2, their expression is determined by the cellular context. In the case of *Myog*, the loss of Wnt signaling leads to the inhibition of *Myod1*, which is needed to activate *Myog* [30]. For *Rb1*, our results show that the sustained expression of cyclin D1 and cyclin E1 leads to the phosphorylation and inactivation of *Rb1*. Clearly, the roles of JARID2 and the PRC2 complex are complex in skeletal muscle and serve to both inhibit and activate several steps of the myogenic program. The direct repression of *Ccnd1* and *Ccne1* by the PRC2 complex in skeletal muscle is especially relevant given that conditional expression of Cdk4/cyclin D1 was recently shown to expand neural stem cells and increase neurogenesis [47]. The authors suggest that this approach could be applied to any tissue to control the expansion of somatic stem cells. In other work, it has also been shown that a combination of cell cycle regulators that includes *Ccnd1* induces cytokinesis in adult postmitotic cardiac cells, revealing that expression of these genes could allow proliferation in cells that had exited the cell cycle and stimulate cardiac regeneration [48]. Our work shows that modulating EZH2 activity regulates Cdk4/cyclin D1, suggesting that this could be used to expand the muscle stem cell pool and enhance skeletal muscle repair and regeneration. Elucidating the multifaceted roles of the PRC2 complex in skeletal muscle contributes to our understanding of normal myogenesis, repair, and disease.

Acknowledgments

We thank Dr. Vjollca Knjufca (Southern Illinois University) for the use of her BD Accuri C6 flow cytometer and Dr. Savannah Howe (Knjufca lab) for her technical expertise and assistance in using this machine. Dr. D. Cornelison (University of Missouri) is thanked for sharing technical advice and reagents for primary myoblast culture. The research reported in this publication

was supported by the National Institute of Arthritis and Musculoskeletal and Skin Diseases of the National Institutes of Health under Award Number RAR068622. The content is solely the responsibility of the authors and does not necessarily represent the official views of the National Institutes of Health.

Disclosure statement

The authors declare that they have no conflicts of interest with the contents of this article.

Funding

This work was supported by the National Institute of Arthritis and Musculoskeletal and Skin Diseases [RAR068622].

ORCID

Abhinav Adhikari  <http://orcid.org/0000-0002-9228-480X>
Judith K. Davie  <http://orcid.org/0000-0003-0458-6646>

References

- [1] Miller JB, Schaefer L, Dominov JA. Seeking muscle stem cells. *Curr Top Dev Biol.* 1999;43:191–219.
- [2] Stockdale FE. Myogenic cell lineages. *Dev Biol.* 1992;154:284–298.
- [3] Shen X, Collier JM, Hlaing M, et al. Genome-wide examination of myoblast cell cycle withdrawal during differentiation. *Dev Dyn.* 2003;226:128–138.
- [4] Berkes CA, Tapscott SJ. MyoD and the transcriptional control of myogenesis. *Semin Cell Dev Biol.* 2005;16:585–595.
- [5] Lassar AB, Skapek SX, Novitch B. Regulatory mechanisms that coordinate skeletal muscle differentiation and cell cycle withdrawal. *Curr Opin Cell Biol.* 1994;6:788–794.
- [6] Molkentin JD, Olson EN. Combinatorial control of muscle development by basic helix-loop-helix and MADS-box transcription factors. *Proc Natl Acad Sci U S A.* 1996;93:9366–9373.
- [7] Geng Y, Yu Q, Sicinska E, et al. Deletion of the p27Kip1 gene restores normal development in cyclin D1-deficient mice. *Proc Natl Acad Sci U S A.* 2001;98:194–199.
- [8] Hitomi M, Stacey DW. Cyclin D1 production in cycling cells depends on ras in a cell-cycle-specific manner. *Curr Biol.* 1999;9:1075–1084.
- [9] Huh MS, Parker MH, Scime A, et al. Rb is required for progression through myogenic differentiation but not

- maintenance of terminal differentiation. *J Cell Biol.* **2004**;166:865–876.
- [10] Blais A, van Oevelen CJ, Margueron R, et al. Retinoblastoma tumor suppressor protein-dependent methylation of histone H3 lysine 27 is associated with irreversible cell cycle exit. *J Cell Biol.* **2007**;179:1399–1412.
- [11] Macaluso M, Montanari M, Giordano A. Rb family proteins as modulators of gene expression and new aspects regarding the interaction with chromatin remodeling enzymes. *Oncogene.* **2006**;25:5263–5267.
- [12] Lundberg AS, Weinberg RA. Functional inactivation of the retinoblastoma protein requires sequential modification by at least two distinct cyclin-cdk complexes. *Mol Cell Biol.* **1998**;18:753–761.
- [13] Bracken AP, Ciro M, Cocito A, et al. E2F target genes: unraveling the biology. *Trends Biochem Sci.* **2004**;29:409–417.
- [14] Cao R, Tsukada Y, Zhang Y. Role of Bmi-1 and Ring1A in H2A ubiquitylation and Hox gene silencing. *Mol Cell.* **2005**;20:845–854.
- [15] Cao R, Wang L, Wang H, et al. Role of histone H3 lysine 27 methylation in Polycomb-group silencing. *Science.* **2002**;298:1039–1043.
- [16] Kuzmichev A, Nishioka K, Erdjument-Bromage H, et al. Histone methyltransferase activity associated with a human multiprotein complex containing the Enhancer of Zeste protein. *Genes Dev.* **2002**;16:2893–2905.
- [17] Muller J, Hart CM, Francis NJ, et al. Histone methyltransferase activity of a Drosophila Polycomb group repressor complex. *Cell.* **2002**;111:197–208.
- [18] Conerly ML, MacQuarrie KL, Fong AP, et al. Polycomb-mediated repression during terminal differentiation: what don't you want to be when you grow up? *Genes Dev.* **2011**;25:997–1003.
- [19] Juan AH, Derfoul A, Feng X, et al. Polycomb EZH2 controls self-renewal and safeguards the transcriptional identity of skeletal muscle stem cells. *Genes Dev.* **2011**;25:789–794.
- [20] Woodhouse S, Pugazhendhi D, Brien P, et al. Ezh2 maintains a key phase of muscle satellite cell expansion but does not regulate terminal differentiation. *J Cell Sci.* **2013**;126:565–579.
- [21] Seale P, Sabourin LA, Girgis-Gabardo A, et al. Pax7 is required for the specification of myogenic satellite cells. *Cell.* **2000**;102:777–786.
- [22] Oustanina S, Hause G, Braun T. Pax7 directs postnatal renewal and propagation of myogenic satellite cells but not their specification. *Embo J.* **2004**;23:3430–3439.
- [23] Olguin HC, Olwin BB. Pax-7 up-regulation inhibits myogenesis and cell cycle progression in satellite cells: a potential mechanism for self-renewal. *Dev Biol.* **2004**;275:375–388.
- [24] Mozzetta C, Consalvi S, Saccone V, et al. Selective control of Pax7 expression by TNF-activated p38alpha/polycomb repressive complex 2 (PRC2) signaling during muscle satellite cell differentiation. *Cell Cycle.* **2011**;10:191–198.
- [25] Palacios D, Mozzetta C, Consalvi S, et al. TNF/p38alpha/polycomb signaling to Pax7 locus in satellite cells links inflammation to the epigenetic control of muscle regeneration. *Cell Stem Cell.* **2010**;7:455–469.
- [26] Acharyya S, Sharma SM, Cheng AS, et al. TNF inhibits Notch-1 in skeletal muscle cells by Ezh2 and DNA methylation mediated repression: implications in duchenne muscular dystrophy. *PloS One.* **2010**;5:e12479.
- [27] von Schimmelmann M, Feinberg PA, Sullivan JM, et al. Polycomb repressive complex 2 (PRC2) silences genes responsible for neurodegeneration. *Nat Neurosci.* **2016**;19:1321–1330.
- [28] Su CL, Deng TR, Shang Z, et al. JARID2 inhibits leukemia cell proliferation by regulating CCND1 expression. *Int J Hematol.* **2015**;102:76–85.
- [29] Iovino N, Ciabrelli F, Cavalli G. PRC2 controls Drosophila oocyte cell fate by repressing cell cycle genes. *Dev Cell.* **2013**;26:431–439.
- [30] Adhikari A, Davie J. JARID2 and the PRC2 complex regulate skeletal muscle differentiation through regulation of canonical Wnt signaling. *Epigenetics Chromatin.* **2018**;11:46.
- [31] Adhikari A, Mainali P, Davie JK. JARID2 and the PRC2 complex regulates the cell cycle in skeletal muscle. *J Biol Chem.* **2019**;294:19451–19464.
- [32] Rando TA, Blau HM. Primary mouse myoblast purification, characterization, and transplantation for cell-mediated gene therapy. *J Cell Biol.* **1994**;125:1275–1287.
- [33] Londhe P, Davie JK. Sequential association of myogenic regulatory factors and E proteins at muscle-specific genes. *Skelet Muscle.* **2011**;1:14.
- [34] Bracken AP, Pasini D, Capra M, et al. EZH2 is downstream of the pRB-E2F pathway, essential for proliferation and amplified in cancer. *Embo J.* **2003**;22:5323–5335.
- [35] Shirato H, Ogawa S, Nakajima K, et al. A jumonji (Jarid2) protein complex represses cyclin D1 expression by methylation of histone H3-K9. *J Biol Chem.* **2009**;284:733–739.
- [36] Asp P, Blum R, Vethantham V, et al. Genome-wide remodeling of the epigenetic landscape during myogenic differentiation. *Proc Natl Acad Sci U S A.* **2011**;108:E149–58.
- [37] Connell-Crowley L, Harper JW, Goodrich DW. Cyclin D1/Cdk4 regulates retinoblastoma protein-mediated cell cycle arrest by site-specific phosphorylation. *Mol Biol Cell.* **1997**;8:287–301.

- [38] Juan AH, Kumar RM, Marx JG, et al. Mir-214-dependent regulation of the polycomb protein Ezh2 in skeletal muscle and embryonic stem cells. *Mol Cell*. 2009;36:61–74.
- [39] Caretti G, Di Padova M, Micales B, et al. The Polycomb Ezh2 methyltransferase regulates muscle gene expression and skeletal muscle differentiation. *Genes Dev*. 2004;18:2627–2638.
- [40] Wong CF, Tellam RL. MicroRNA-26a targets the histone methyltransferase Enhancer of Zeste homolog 2 during myogenesis. *J Biol Chem*. 2008;283:9836–9843.
- [41] Pajcini KV, Corbel SY, Sage J, et al. Transient inactivation of Rb and ARF yields regenerative cells from postmitotic mammalian muscle. *Cell Stem Cell*. 2010;7:198–213.
- [42] McCabe MT, Ott HM, Ganji G, et al. EZH2 inhibition as a therapeutic strategy for lymphoma with EZH2-activating mutations. *Nature*. 2012;492:108–112.
- [43] Piunti A, Shilatifard A. Epigenetic balance of gene expression by Polycomb and COMPASS families. *Science (New York, NY)*. 2016;352:aad9780.
- [44] Piunti A, Rossi A, Cerutti A, et al. Polycomb proteins control proliferation and transformation independently of cell cycle checkpoints by regulating DNA replication. *Nat Commun*. 2014;5:3649.
- [45] Singh K, Dilworth FJ. Differential modulation of cell cycle progression distinguishes members of the myogenic regulatory factor family of transcription factors. *FEBS J*. 2013;280:3991–4003.
- [46] Gan L, Yang Y, Li Q, et al. Epigenetic regulation of cancer progression by EZH2: from biological insights to therapeutic potential. *Biomark Res*. 2018;6:10.
- [47] Bragado Alonso S, Reinert JK, Marichal N, et al. An increase in neural stem cells and olfactory bulb adult neurogenesis improves discrimination of highly similar odorants. *Embo J*. 2019;38.
- [48] Mohamed TMA, Ang YS, Radzinsky E, et al. Regulation of cell cycle to stimulate adult cardiomyocyte proliferation and cardiac regeneration. *Cell*. 2018;173:104–16 e12.